Phase-bistable patterns and cavity solitons induced by spatially periodic injection into vertical-cavity surface-emitting lasers

C. Fernandez-Oto,[1] G. J. de Valcárcel,[2] M. Tlidi,[1] K. Panajotov,[3,4] and K. Staliunas[5,6]

[1]*Faculté des Sciences, Université Libre de Bruxelles (U. L. B.), C. P. 231, Campus Plaine, B-1050 Bruxelles, Belgium*

[2]*Departament d'Òptica, Universitat de València, Dr. Moliner 50, E-46100 Burjassot, Spain*

[3]*Brussels Photonics Team, Department of Applied Physics and Photonics (B-PHOT TONA), Vrije Unversiteit Brussels, Pleinlaan 2, B-1050 Brussels, Belgium*

[4]*Institute of Solid State Physics, 72 Tzarigradsko Chaussee Blvd., B-1784 Sofia, Bulgaria*

[5]*Departament de Física i Enginyeria Nuclear, Universitat Politècnica de Catalunya, Colom 11, E-08222 Terrassa (Barcelona), Spain*

[6]*Institució Catalana de Recerca i Estudis Avançats (ICREA), Pg. Lluís Companys 23, E-08010 Barcelona, Spain*

(Received 7 February 2014; published 8 May 2014)

Spatial rocking is a kind of resonant forcing able to convert a self-oscillatory system into a phase-bistable, pattern forming system, whereby the phase of the spatially averaged oscillation field locks to one of two values differing by π. We propose the spatial rocking in an experimentally relevant system—the vertical-cavity surface-emitting laser (VCSEL)—and demonstrate its feasibility through analytical and numerical tools applied to a VCSEL model. We show phase bistability, spatial patterns, such as roll patterns, domain walls, and phase (dark-ring) solitons, which could be useful for optical information storage and processing purposes.

DOI: 10.1103/PhysRevA.89.055802 PACS number(s): 42.65.Sf, 42.65.Tg, 05.65.+b, 05.45.−a

Introduction. Many nonlinear open systems exhibit spontaneous pattern formation when maintained far away from their thermodynamic equilibrium [1,2]. One of the most remarkable examples of such behavior is the emergence of localized structures (LSs) and lalized patterns that have been predicted and observed in a wide variety of systems [3]. Controlling such dissipative structures is one of the central issues in nonlinear science. In particular, several types of periodic forcing, in time and/or in space, have been proposed in literature [4–12]. The periodic forcing in time can generate different resonances associated with the natural frequency of the system. An alternative type of forcing (coined "rocking"), characterized by a fundamental temporal frequency close to the system's natural frequency (1:1 resonance in the terminology of forced nonlinear oscillators), but with a special kind of modulated amplitude, has been proposed [13,14]. That modulation must entail sign alternations (i.e., π-phase jumps) of the forcing in time (temporal rocking) or in space (spatial rocking) and must occur on sufficiently fast, nonresonant scales as compared to the typical scales of the oscillations' envelope dynamics. Theoretical [13–19] and experimental [16,20,21] studies have revealed that this type of forcing converts the initially phase-invariant oscillatory system into a phase-bistable pattern forming one, similarly to the classic 2:1 resonant forcing (at twice the system's natural frequency) of a spatially homogeneous Hopf bifurcation [8,9]. The advantage of rocking with respect to the 2:1 resonance is that some systems (optical in particular) are insensitive to the latter, due to their extremely narrow frequency response. Hence rocking is the actual alternative to the 2:1 resonant forcing in optical systems if one wishes to excite phase-bistable patterns, which are especially interesting because, on one hand, they can be of topological nature—making them very robust—and, on the other hand, allow codification of information in phase bits. Rocking is a universal phenomenon as it is not critically system dependent; in fact, the initial theoretical proposals [13,14] used complex Ginzburg-Landau models, which are the universal description for a system close to a spatially homogeneous Hopf bifurcation, to reveal the phenomena described above. In the optical arena, rocking of small Fresnel number (small aspect ratio) nonlinear resonators results in a global phase bistability affecting the whole light beam [15,20], while for large Fresnel number systems more spatial degrees of freedom are available and rocking leads to the excitation of spatial phase-bistable patterns that form on the transverse section of the light beam, such as phase domains, rolls, and phase solitons [13,14]. In particular, spatial rocking, which is the concern of the present study, has been considered in a one-transverse-dimensional broad area semiconductor laser [17] and in a Kerr resonator [19].

In this paper we provide theoretical (analytical and numerical) evidence that spatial rocking (realized through resonant, spatially structured optical injection) is feasible in vertical-cavity surface-emitting lasers (VCSELs). These semiconductor-based devices have potential applications for all-optical control of light, optical information storage, and processing [22–24]. In particular, the fast time response of VCSELs makes them attractive for applications in all optical delay lines [25], and logic gates [26]. We investigate a well-established model for pattern formation in VCSELs with optical injection [27], using experimentally accessible parameters. We demonstrate a variety of phase-bistable spatial patterns stabilized by the spatially periodic modulated injection. The spatial scale of the patterns depends on the effective detuning, in accordance with general principles of pattern formation due to detuned forcing [8].

Model. We adopt a well-established model for studying localized structures, also called cavity solitons, in optically injected VCSELs [27]. This model describes the coupled space-time evolution of the electric field envelope E and the carrier density D and is given by the following set of dimensionless partial differential equations,

$$\begin{aligned}\partial_t E(\mathbf{r},t) &= -[1+i\theta+2C(i\alpha-1)D-i\nabla^2]E+E_I(\mathbf{r}),\\ \partial_t D(\mathbf{r},t) &= -\gamma[(1+|E|^2)D-1-d\nabla^2 D].\end{aligned} \tag{1}$$

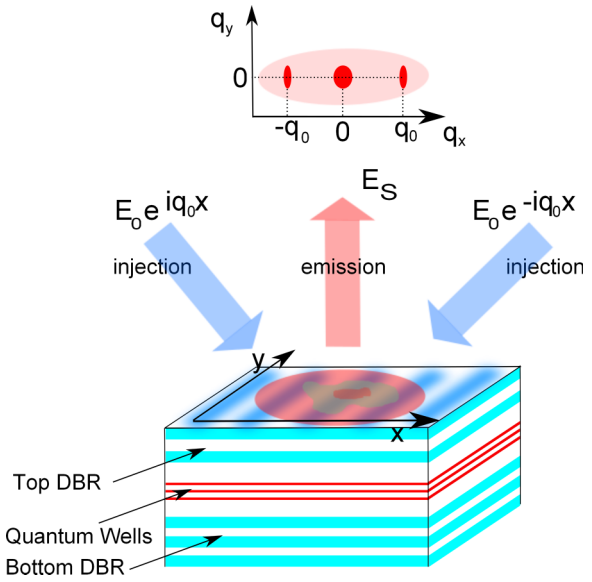

FIG. 1. (Color online) VCSEL with spatially periodic injection. As an example the 1D modulation of injection is shown, which can be realized by interference of two beams. Inset illustrates the expected patterns in far-field domain.

Here t denotes time normalized to the cavity decay rate and $\mathbf{r} = (x, y)$ denotes the transverse coordinates normalized to the diffraction length. The cavity detuning from the input field frequency is measured by θ; α is the linewidth enhancement factor of semiconductors; d is the ratio of the diffusion to diffraction coefficients; γ is the carrier decay rate; and C is the pump parameter, proportional to the injected current ($C = 0.5$ corresponds to the lasing threshold). We omitted a term in Eq. (1) describing radiative recombination because of its weak influence on the results [27]. The diffusion coefficient d in VCSELs is small, and carrier diffusion can indeed be neglected in the case of quantum well lasers [28]. For spatial rocking to occur, the injected field E_I is not constant as in [27], but rather a periodic function of space, e.g., $E_I(\mathbf{r}) = E_x \cos(q_x x) + E_y \cos(q_y y)$. This spatially periodic injection can be experimentally realized by coherently interfering beams injected at different angles as illustrated in Fig. 1. In all cases we deal with injected fields whose spatial average is null [14]. We consider both one-dimensional (1D) injection ($E_x = E_0, E_y = 0, q_x = q_0$) and two-dimensional (2D) injection ($E_x = E_y = E_0, q_x = q_y = q_0$).

Steady states. Some indications of rocking can be obtained by considering the steady states of the system. Setting the time derivatives in Eq. (1) to zero and neglecting carrier diffusion the following equation for the field envelope can be derived:

$$\left[1 + i\theta + \frac{2C(i\alpha - 1)}{1 + |E|^2} - i\nabla^2\right] E(\mathbf{r}) = E_I(\mathbf{r}). \qquad (2)$$

We further assume that the injected field is modulated on a sufficiently short spatial scale so that the field can be decomposed as $E(\mathbf{r}) = E_f(\mathbf{r}) + E_s(\mathbf{r})$ to a good approximation, where $E_f(\mathbf{r})$ is a "fast" component (displaying spatial variations on the scale of the injected field) and $E_s(\mathbf{r})$ is a "slow" component, varying on the (comparatively long) scale of the unforced system [4]. Substituting that decomposition into Eq. (2) and separating terms related with small and large spatial frequencies, one finds that the dominant contribution to E_f comes from diffraction, hence $\nabla^2 E_f(\mathbf{r}) = i E_I(\mathbf{r})$ to a good approximation. For the slow part one obtains

$$(1 + i\theta - i\nabla^2)E_s + 2C(i\alpha - 1)\left\langle \frac{E_f + E_s}{1 + |E_f + E_s|^2} \right\rangle = 0, \qquad (3)$$

where the angular brackets denote a spatial averaging over the fast scale (thus $\langle E_s \rangle = E_s$). As we wish that $E_s = 0$ is a solution (otherwise we would have a mixed dynamics where some features of the usual laser with injected signal would appear thus completely breaking the phase symmetry of the emission), Eq. (3) imposes a condition on the injected field E_I through E_f, namely $\langle E_f/(1 + |E_f|^2) \rangle = 0$.

To fix ideas we focus first on the 1D case, in which $E_f(\mathbf{r}) = -i\sqrt{F}\cos(q_0 x)$ with $F = (E_0/q_0^2)^2$ and we took $E_0 > 0$ without loss of generality. F is an effective rocking parameter which we will use in the following. The averaging in Eq. (3) can be worked out analytically, with the result,

$$(1 + i\theta - i\nabla^2)E_s + 2C(i\alpha - 1) \times \left[\frac{X_s}{\sqrt{1 + X_s^2}} \mathrm{Re}\left(\frac{1}{\sqrt{A}}\right) + i\,\mathrm{Im}\left(\frac{1}{\sqrt{A}}\right)\right] = 0, \qquad (4)$$

where $X_s = \mathrm{Re}(E_s)$, $Y_s = \mathrm{Im}(E_s)$, and $A = F + (\sqrt{1 + X_s^2} - iY_s)^2$. Equation (4) does not hold the continuous phase symmetry $E_s \to E_s \exp(i\phi)$ but is invariant under the discrete transformation $E_s \to -E_s$. The main effect of rocking, namely the existence of two equivalent, opposite phases [14] is thus revealed by Eq. (4). In addition Eq. (4) determines any steady-state solution of the system. An explicit expression for the dynamical evolution of the homogeneous steady state E_s is out of the scope of this paper. However, one can compute the condition of existence of a nonzero, spatially uniform slow field component. Dividing Eq. (3) by E_s, expressing E_s in polar form and taking in the resulting equation the limit $R = |E_s| \to 0$, the following equation for the rocking boundary is obtained:

$$4C^2(1 + \alpha^2) + 2C(\alpha\theta - 1)(2 + F)\sqrt{1 + F} + (1 + \theta^2)(1 + F)^2 = 0. \qquad (5)$$

This equation determines where the "rocked," spatially uniform solutions ($E_s = \text{const.}$) bifurcate from the off state.

Small aspect ratio system. In order to prove the impact of the rocking on the homogeneous state (on the slow spatial scale, corresponding to $E_s = \text{const.}$), we first consider a small aspect ratio VCSEL, in which spontaneous spatial pattern formation is impossible. We perform numerical integrations of Eq. (1) in 1D with the same parameters as in Fig. 2, and determine the parametric region where rocking is observed. This region is shown in the plane (F,θ) in the Fig. 2 area formed by dots, together with the analytically obtained from Eq. (5). The results obtained from Eq. (5), in which the diffusion of the carrier density is neglected, and the numerical simulations of full model Eq. (1) are in agreement as shown in Fig. 2. This figure also shows that the numerical results are in good agreement with the analytical ones in the upper part of the rocking balloon. In the lower part of the balloon the steady

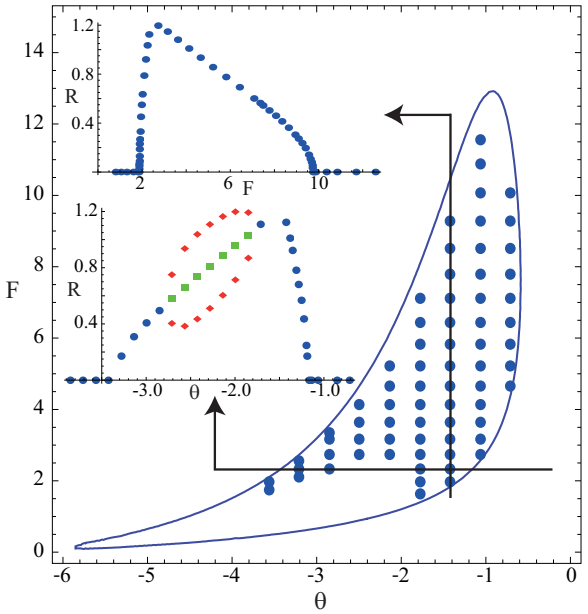

FIG. 2. (Color online) The rocking balloon is shown on the parameter space of frequency detuning θ; injection amplitude F (see text). The parameters are $C = 0.64$, $\alpha = 5.0$, $\gamma = 0.014$, $d = 0.00007$, and $q_0 = 7.5$. The insets represent the intensity of averaged field R in two cross sections: vertical cross section at $\theta = -1.43$ and horizontal cross section at $F = 2.3$.

state ceases to exist as a Hopf bifurcation sets in the system as shown in the inset of Fig. 2. The Hopf bifurcation depends on the carrier relaxation rate γ, however, even for small values of $\gamma \sim 10^{-2}$ the rocking does not disappear. Therefore, our results show that rocking can be experimentally realized in VCSELs with $\gamma \sim 10^{-2}$, as it exists in a sufficiently large parameter area of injection amplitude and frequency detuning.

Large aspect ratio system, 1D injection modulation. Next, we report the spatial patterns emerging on a large space scale. We use different parameter values to illustrate the different spatial patterns. The nondimensionalization used in Eq. (1) is such that an injected field intensity $|E_0|^2 = 1$ corresponds in physical units to 1 kW/cm^2, and a wave number $q_0 = 1$ corresponds in physical units to $0.23/\mu$m. In order to have enough transverse space to form the pattern, we consider a large Fresnel number of order $\sim 10^3$.

The simplest spatial structure of the phase-bistable system is a phase domain boundary: If in the neighboring lateral regions stable solutions with opposite values of the averaged phase are realized, then a domain boundary must appear in between, separating these two phase domains. The domain boundaries obtained by numerical integration are shown in Fig. 3(a). The field oscillations on a small scale are confusing, therefore we plot the field amplitude and the phase of the field averaged over a small size.

In a limited part of the rocking domain the domain walls of opposite polarity can mutually lock, constituting phase solitons shown in Fig. 3(b). The locking range depends on many parameters, like the α parameter and the carrier diffusion coefficient d. Generally speaking the spatial oscillations of the fields due to domain boundaries (exponentially decaying tails)

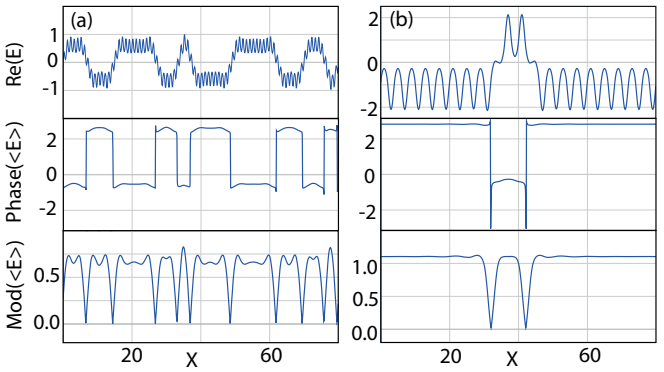

FIG. 3. (Color online) 1D patterns obtained by numerical integration of (1) for periodic injection $E_0 \cos(qx)$: domain walls (a) and phase soliton (b). The parameters in (a) and (b) are $C = 0.64$, $\alpha = 5.0$, $\gamma = 0.01$, and $d = 0.0001$. In (a) $\theta = -1.3$, $E_0 = 25.0$, and $q_0 = \pi$. In (b) $\theta = -1.2$, $E_0 = 6.0$, and $q_0 = \pi/2$.

are responsible for the locking, and with more pronounced oscillations the locking is more efficient, i.e., the existence domain of the phase solitons is larger [29,30].

Large aspect ratio system, 2D injection modulation. In the 2D case, the morphology of the system becomes more complex. In the following we consider injection of square symmetry ($E_x = E_y = E_0, q_x = q_y = q_0$), which generates squared modulation of the background in the real (or imaginary) part of the field that can be observed in the nonaveraged field in Fig. 4. The 2D phase domains are shown in Fig. 4(a), which are analogous to 1D phase domains in Fig. 3. In the 2D case, this kind of solution is unstable because of the surface tension that affects the dynamics of the phase domains [31]. The surface tension, however, can be either positive or negative for domain walls in a phase-bistable system [30], depending on the off-resonance detuning. We could observe this scenario also in VCSEL with spatial periodic injection, where the detuning parameter θ provides such a control over the surface tension. For smaller absolute values of θ the domain walls are coarsening and the domains are contracting, as shown in Fig. 4(a). For larger absolute values of θ the domains are growing (the structure is anticoarsening), which is related to the negative surface tension of the domain walls [29,30]. This case eventually leads to the labyrinth structure as illustrated in Fig. 4(b). The labyrinth in the 2D spatially extended systems is analogous to a roll pattern in 1D systems.

Finally, in the regime of a positive but weak surface tension, the contracting domains could stop contracting at a definite (a minimum) radius. This stabilization of domains is related with the spatial oscillation of the tails of the domain boundaries like in the above discussed 1D case. Field oscillations from a segment of domain boundary trap the opposite segment of domain boundary in accordance with [32]. This leads to stable, round, phase solitons, in the form of dark rings of field intensity, as shown in Figs. 4(c) and 4(d). The phase solitons in two dimensions are analogous to the phase solitons in one dimension shown in Fig. 3(b). Due to the absence of surface tension in the 1D case, the existence ranges of the 1D and 2D solitons are slightly shifted with respect to each other in the parameter space.

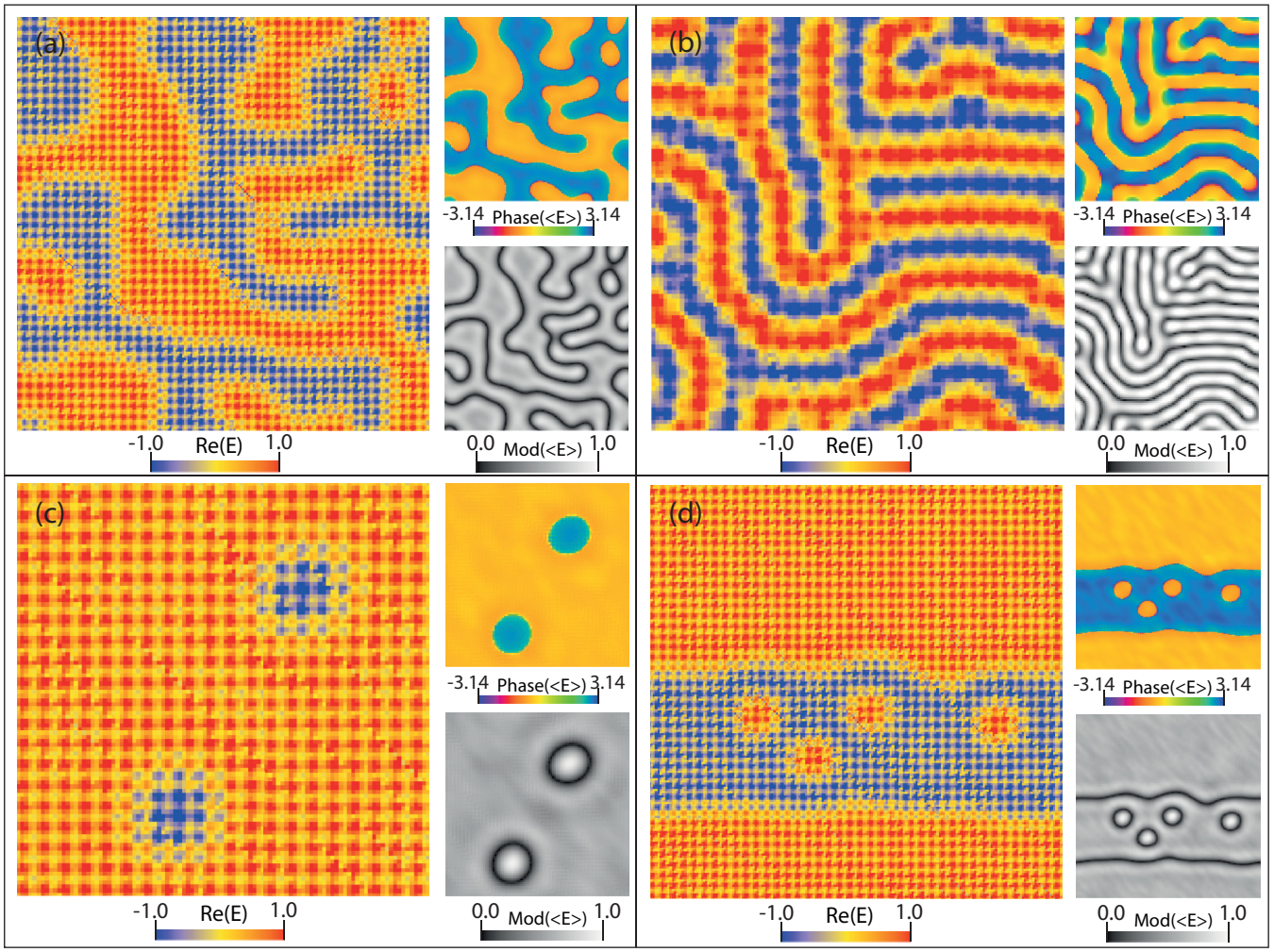

FIG. 4. (Color online) 2D patterns as obtained by numerical integration of (1) in the two-dimensional case: domain walls (a), labyrinth patterns (corresponding to rolls in 1D) (b), dark-ring solitons (c), and coexisting domain walls and solitons (d). The parameters in (a), (b), (c), and (d) are $C = 0.8$, $\alpha = 5.0$, $\gamma = 0.01$, $d = 0.0001$, and $q_0 = \pi$. In (a) $\theta = -1.6$ and $E_0 = 22.0$. In (b) $\theta = -2.7$ and $E_0 = 14.0$. In (c) $\theta = -1.7$ and $E_0 = 22.0$. In (d) $\theta = -1.65$ and $E_0 = 22.0$.

Conclusion. We have studied theoretically and numerically broad area VCSEL with spatially periodic injection modulated in one and two dimensions. We show that the spatial rocking phenomenon can be realized in VCSELs at an experimentally accessible parameter range. We show that, generally, the rocking balloon depends on the time scales of the coupled fields. Small values of $\gamma \ll 1$ reduce the size of the rocking balloon, however, the balloon does not shrink to zero. This allows one to obtain the rocking with experimentally realistic parameters ($\gamma \sim 10^{-2}$ and $E_0 \sim 10$). On the other hand, when the system is larger, it is possible to observe different kinds of spatial structures. In 1D and 2D extended systems we observed a variety of patterns, phase domains, phase solitons, rolls, and labyrinth structures.

Acknowledgments. C.F.-O. acknowledges financial support from Becas Chile. M.T. received support from the Fonds National de la Recherche Scientifique (Belgium). G.deV. and K.S. acknowledge financial support from the Spanish Government and European FEDER (Projects No. FIS2011-29734-C02-01 and No. FIS2011-26960). M.T. and K.P. acknowledge financial support from the Interuniversity Attraction Poles program of the Belgian Science Policy Office, under Grant No. IAP 7-35.

[1] P. Glansdorff and I. Prigogine, *Thermodynamic Theory of Structures, Stability and Fluctuations* (Wiley, New York, 1971).

[2] I. Prigogine and R. Lefever, J. Chem. Phys. **48**, 1695 (1968).

[3] N. N. Rosanov, Prog. Opt. **35**, 1 (1996); D. Mihalache *et al.*, *ibid.* **27**, 227 (1989); N. N. Rosanov, *Spatial Hysteresis and Optical Patterns* (Springer, Berlin, 2002); K. Staliunas and V. J. Sánchez-Morcillo, *Transverse Patterns in Nonlinear Optical Resonators* (Springer Tracts in Modern Physics) (Springer-Verlag, Berlin, 2003); P. Mandel and M. Tlidi, J. Opt. B **6**, R60 (2004); N. Akhmediev and A. Ankiewicz, *Dissipative Solitons: From Optics to Biology and Medicine* (Springer-Verlag, Berlin/Heidelberg, 2008); O. Descalzi, M. Clerc, S. Residori, and G. Assanto, *Localized States in Physics: Solitons and Patterns* (Springer, New York, 2011).

[4] P. L. Kapitza, Sov. Phys. JETP **21**, 588 (1951) [in Russian]; see also in *Collected Papers of P. L. Kapitza*, edited by D. Ter Haar (Pergamon, London, 1965), p. 714; L. D. Landau and E. M. Lifshiftz, *Mechanics* (Pergamon, Oxford, 1976).
[5] M. G. Clerc, C. Falcon, C. Fernandez-Oto, and E. Tirapegui, Europhys. Lett. **98**, 30006 (2012); M. G. Clerc, C. Fernandez-Oto, and S. Coulibaly, Phys. Rev. E **87**, 012901 (2013).
[6] Y. S. Kivshar, N. Grønbech-Jensen, and M. R. Samuelsen, Phys. Rev. B **45**, 7789 (1992).
[7] A. Frova and M. Marenzana, *Thus Spoke Galileo: The Great Scientist's Ideas and their Relevance to the Present Day* (Oxford University Press, Oxford, 2006).
[8] P. Coullet, J. Lega, B. Houchmanzadeh, and J. Lajzerowicz, Phys. Rev. Lett. **65**, 1352 (1990); P. Coullet and K. Emilsson, Physica D **61**, 119 (1992).
[9] V. Petrov, Q. Ouyang, and H. L. Swinney, Nature (London) **388**, 655 (1997); A. L. Lin, M. Bertram, K. Martinez, H. L. Swinney, A. Ardelea, and G. F. Carey, Phys. Rev. Lett. **84**, 4240 (2000).
[10] C. Elphick, A. Hagberg, E. Meron, and B. Malomed, Phys. Lett. A **230**, 33 (1997); A. G. Vladimirov, D. V. Skryabin, G. Kozyreff, P. Mandel, and M. Tlidi, Opt. Express **14**, 1 (2006); Y. Mau, L. Haim, A. Hagberg, and E. Meron, Phys. Rev. E **88**, 032917 (2013).
[11] R. Neubecker and A. Zimmermann, Phys. Rev. E **65**, 035205(R) (2002).
[12] S. Rüdiger, E. M. Nicola, J. Casademunt, and L. Kramer, Phys. Rep. **447**, 73 (2007).
[13] G. J. de Valcárcel and K. Staliunas, Phys. Rev. E **67**, 026604 (2003).
[14] G. J. de Valcárcel and K. Staliunas, Phys. Rev. Lett. **105**, 054101 (2010).
[15] K. Staliunas, G. J. de Valcárcel, and E. Roldán, Phys. Rev. A **80**, 025801 (2009).
[16] K. Staliunas, G. J. de Valcárcel, J. M. Buldú, and J. García-Ojalvo, Phys. Rev. Lett. **102**, 010601 (2009).
[17] M. Radziunas and K. Staliunas, Europhys. Lett. **95**, 14002 (2011).
[18] K. Staliunas *et al.*, Opt. Commun. **268**, 160 (2006).
[19] G. J. de Valcárcel and K. Staliunas, Phys. Rev. A **87**, 043802 (2013).
[20] S. Kolpakov, F. Silva, G. J. de Valcárcel, E. Roldán, and K. Staliunas, Phys. Rev. A **85**, 025805 (2012).
[21] A. Esteban-Martín, M. Martínez-Quesada, V. B. Taranenko, E. Roldán, and G. J. de Valcárcel, Phys. Rev. Lett. **97**, 093903 (2006).
[22] V. B. Taranenko, K. Staliunas, and C. O. Weiss, Phys. Rev. A **56**, 1582 (1997).
[23] S. Barland, J. R. Tredicce, M. Brambilla, L. A. Lugiato, S. Balle, M. Giudici, T. Maggipinto, L. Spinelli, G. Tissoni, T. Knödl, M. Miller, and R. Jäger, Nature (London) **419**, 699 (2002).
[24] X. Hachair *et al.*, Phys. Rev. A **69**, 043817 (2004); X. Hachair, G. Tissoni, H. Thienpont, and K. Panajotov, *ibid.* **79**, 011801 (2009).
[25] F. Pedaci *et al.*, Appl. Phys. Lett. **92**, 011101 (2008).
[26] A. Jacobo, D. Gomila, M. A. Matias, and P. Colet, New J. Phys. **14**, 013040 (2012).
[27] M. Brambilla, L. A. Lugiato, F. Prati, L. Spinelli, and W. J. Firth, Phys. Rev. Lett. **79**, 2042 (1997).
[28] F. Prati, A. Tesei, L. A. Lugiato, and R. J. Horowicz, Chaos, Solitons & Fractals **4**, 1637 (1994).
[29] V. B. Taranenko, K. Staliunas, and C. O. Weiss, Phys. Rev. Lett. **81**, 2236 (1998); M. Tlidi, P. Mandel, and R. Lefever, *ibid.* **81**, 979 (1998); M. Tlidi, Paul Mandel, M. Le Berre, E. Ressayre, A. Tallet, and L. Di Menza, Opt. Lett. **25**, 487 (2000).
[30] K. Staliunas and V. J. Sánchez-Morcillo, Phys. Lett. A **241**, 28 (1998); D. Gomila, P. Colet, G.-L. Oppo, and M. San Miguel, Phys. Rev. Lett. **87**, 194101 (2001).
[31] L. D. Landau and E. M. Lifshiftz, *Course of Theoretical Physics, Vol. 6: Fluid Mechanics* (Pergamon Press, Oxford, 1959); T. A. Witten and P. A. Pincus, *Structured Fluids* (Oxford University Press, Oxford, 2010).
[32] V. J. Sánchez-Morcillo and K. Staliunas, Phys. Rev. E **60**, 6153 (1999); K. Staliunas and V. J. Sánchez-Morcillo, Phys. Rev. A **57**, 1454 (1998).